Key Points:
- Entrainment-limited uptake provides a new, realistic representation of cloud chemistry for atmospheric models that do not resolve clouds
- Clouds reduce global tropospheric NO_x, O_3, and OH through uptake of NO_3 and N_2O_5
- Accounting for cloud chemistry reduces the sensitivity of tropospheric oxidants to aerosol heterogeneous chemistry

The Role of Clouds in the Tropospheric NO_x Cycle: A New Modeling Approach for Cloud Chemistry and Its Global Implications

Christopher D. Holmes[1] (iD), Timothy H. Bertram[2] (iD), Kaitlyn L. Confer[1], Kelly A. Graham[1], Allison C. Ronan[1], Charles K. Wirks[1], and Viral Shah[3] (iD)

[1]Department of Earth, Ocean, and Atmospheric Science, Florida State University, Tallahassee, FL, USA, [2]Department of Chemistry, University of Wisconsin, Madison, WI, USA, [3]Harvard John A. Paulson School of Engineering and Applied Sciences, Harvard University, Cambridge, MA, USA

Abstract We present a new method for simulating heterogeneous (surface and multiphase) cloud chemistry in atmospheric models that do not spatially resolve clouds. The method accounts for cloud entrainment within the chemical rate expression, making it more accurate and stable than other approaches. Using this "entrainment-limited uptake," we evaluate the role of clouds in the tropospheric NO_x cycle. Past literature suggests that on large scales, losses of N_2O_5 and NO_3 in clouds are much less important than losses on aerosols. We find, however, that cloud reactions provide 25% of tropospheric NO_x loss in high latitudes and 5% of global loss. Homogeneous, gas phase hydrolysis of N_2O_5 is likely 2% or less of global NO_x loss. Both clouds and aerosols have similar impacts on global tropospheric O_3 and OH levels, around 2% each. Accounting for cloud uptake reduces the sensitivity of atmospheric chemistry to aerosol surface area and uptake coefficient since clouds and aerosols compete for the same NO_3 and N_2O_5.

Plain Language Summary Cloud water droplets and ice crystals enable some aqueous and surface chemical reactions that otherwise would not occur in the gaseous atmosphere. While clouds are widespread and familiar, methods for simulating their multiphase chemical effects in global atmospheric models have been inadequate. We present an efficient mathematical method to represent the combined effects of cloud chemistry and entrainment in large-scale atmospheric chemistry models that do not resolve individual clouds. By applying the approach to nitrogen oxides, we show that clouds have a previously unrecognized impact on tropospheric ozone, an air pollutant and greenhouse gas, and hydroxyl, a key atmospheric oxidant.

1. Introduction

Nitrogen oxides (NO_x = NO + NO_2) play a critical role in tropospheric chemistry, by catalyzing the chemical production of key oxidants—O_3 and OH—during hydrocarbon oxidation. NO_x is emitted into the atmosphere by combustion, lightning, and soil microbes and removed mainly as nitric acid (HNO_3), which is efficiently scavenged in dry and wet deposition (Logan, 1983). Most HNO_3 forms through the reaction of NO_2 with OH; however, hydrolysis of N_2O_5 on aerosol and cloud surfaces is an important secondary pathway (Alexander et al., 2009; Dentener & Crutzen, 1993). While past literature suggests that tropospheric N_2O_5 loss on clouds are small on regional and global scales compared to loss on aerosol (Dentener & Crutzen, 1993; Jacob, 2000), this work revisits the role of clouds in light of our improved understanding of reactive chemistry on tropospheric aerosol.

N_2O_5, which is produced through reactions between NO_2 and NO_3, is a nighttime reservoir of NO_x (Atkinson et al., 1986; Brown et al., 2003; Chang et al., 2011; Platt & Janssen, 1995). N_2O_5 decomposes at warm temperatures and under sunlight, but its main loss in the lower troposphere is hydrolysis in aerosol and cloud water (Brown et al., 2007; Heikes & Thompson, 1983). The hydrolysis product is HNO_3, which typically remains particle bound, although gaseous $ClNO_2$ is possible in particles with high salt content (Behnke et al., 1997; Bertram & Thornton, 2009; Finlayson-Pitts et al., 1989; Thornton & Abbatt, 2005; Thornton et al., 2010). Heterogeneous reaction rates, including surface and multiphase reactions, are controlled by mass transfer from the gas phase to liquid surfaces and details of surface or aqueous chemistry can be encapsulated in a reactive uptake coefficient, γ, that represents the reaction probability for a molecule impacting

the cloud or aerosol surface (Jacob, 2000; Ravishankara, 1997; Sander, 1999; Schwartz, 1986). For cloud water, $\gamma_{N_2O_5} = 0.03$ at 298 K and rises with colder temperatures (Bertram & Thornton, 2009; Burkholder et al., 2015; van Doren et al., 1990). For aerosols, the N_2O_5 uptake coefficient strongly depends on composition (Bertram & Thornton, 2009; Brown et al., 2006; McDuffie et al., 2018), but, with the exception of stratospheric sulfuric acid aerosol, the uptake coefficient is generally less than pure water (Ammann et al., 2013; Burkholder et al., 2015; Crowley, Ammann, et al., 2010). While clouds have greater $\gamma_{N_2O_5}$ and far greater surface area than tropospheric aerosol (around 1,000 times greater surface area; inferred from aerosol, Heald et al., 2014, and cloud, Pruppacher & Jaenicke, 1995, data), their influence on global N_2O_5 and tropospheric chemistry is limited by the small volume occupied by clouds and the intervals of hours to days between cloud contacts (Lelieveld & Crutzen, 1990, 1991).

In atmospheric models, N_2O_5 hydrolysis on aerosols lowers the global tropospheric NO_x burden around 15% and lowers O_3 and OH around 5% each, relative to models without this process (for $\gamma_{N_2O_5} \approx 0.01-0.03$; Evans & Jacob, 2005; Macintyre & Evans, 2010). This aerosol uptake accounts for 8–40% of global HNO_3 production (Alexander et al., 2009; Bauer, 2004; Evans & Jacob, 2005; Hauglustaine et al., 2014; Xu & Penner, 2012). Earlier studies suggested larger impacts but overestimated the uptake coefficient for tropospheric aerosol ($\gamma_{N_2O_5} = 0.1$ was assumed, based on laboratory data available at the time; Dentener & Crutzen, 1993; Liao et al., 2003; Tie et al., 2001). One of the earliest studies concluded that N_2O_5 hydrolysis in cloud water has little impact on tropospheric chemistry, except in the remote southern hemisphere, because in their model, ubiquitous aerosol already consumed most N_2O_5 (Dentener & Crutzen, 1993). As a result, some atmospheric chemistry models neglect N_2O_5 hydrolysis in clouds (Evans & Jacob, 2005; Folberth et al., 2006; Hauglustaine et al., 2014; Tie et al., 2001; Xu & Penner, 2012). However, since their $\gamma_{N_2O_5}$ value was too high in light of more recent laboratory and field studies, Dentener and Crutzen (1993) overestimated the role of aerosols relative to clouds in N_2O_5 hydrolysis and it appears that the importance of clouds in the global NO_x budget has not been revisited since.

In this work, we add N_2O_5 hydrolysis on clouds to a global atmospheric chemistry model and quantify its impact on tropospheric oxidants. Our treatment of cloud uptake of N_2O_5 uses a new mathematical modeling approach, developed in section 2, for treating mass exchange between gas and cloud droplets in a partially cloudy model grid cell. We show that this new approach dramatically reduces errors in the chemical solver relative to existing methods used in global atmospheric chemistry models. Sections 3 and 4 describe the improved model and examine the broader implications for tropospheric chemistry.

2. Reactive Chemical Uptake in Partly Cloudy Conditions

The rate at which aqueous reactions consume gas, such as N_2O_5, within a cloud, fog, or other aerosol, is (Fuchs & Sutugin, 1971; Jacob, 2000; Sander, 1999; Schwartz, 1986)

$$J_i = k_i c_i, \qquad k_i = A \left(\frac{r}{D_g} + \frac{4}{v\gamma} \right)^{-1}. \qquad (1)$$

Here c_i is the gas concentration in interstitial air, A is the surface area density of cloud or aerosol, r is the droplet or aerosol radius, D_g is the diffusivity in air, v is the mean molecular speed, and γ is the reactive uptake coefficient. The surface area density of spherical cloud droplets is related to the liquid water content, L, by $A = 3L/\rho r$, where ρ is the density of water. For typical cloud conditions ($L = 0.3 \text{ g/m}^3, r = 10 \ \mu\text{m}, D_g = 2\times10^{-5} \text{ m}^2/\text{s}, v = 300 \text{ m/s}, \gamma_{N_2O_5} = 0.03$), the characteristic timescale for heterogeneous loss of N_2O_5 inside a cloud is $k_i^{-1} \approx 10$ s. This timescale is much shorter than the residence time of air in clouds, which is 15–120 min for many stratus and cumulus clouds (Feingold et al., 1998, 2013; Kogan, 2004; Lelieveld et al., 1989; Stevens et al., 1996) although it can be longer for cirrus (Podglajen et al., 2016). As a result, N_2O_5 and other gases with fast, irreversible, aqueous loss are depleted in clouds relative to surrounding clear air (Brown et al., 2016; Platt et al., 1981). The loss rate of N_2O_5 and similar gases therefore strongly depends on the rate at which these gases are entrained into the cloud from the surrounding air.

Global atmospheric chemistry models, and some regional models, do not resolve individual clouds or entrainment, so these processes must be parameterized to simulate cloud heterogeneous chemistry.
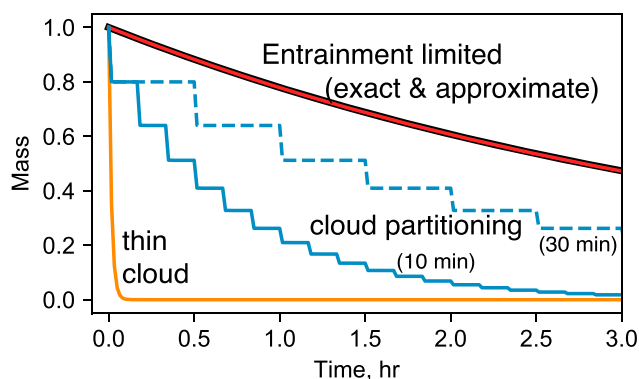
Figure 1. Uptake of a reactive gas ($\gamma = 0.03$) in a partly cloudy environment as simulated with several methods (section 2). The approximate entrainment-limited uptake (equation (4)) matches the exact solution (equations (2) and (3)) within the accuracy of the red and black lines, while the commonly used thin cloud and cloud repartitioning methods predict much faster loss. Time steps for the cloud partitioning method are in parentheses. All methods use the same cloud and chemical conditions: $f_c = 0.2$, $\tau_c = 1$ hr, $L = 0.3$ g/m^3, $r = 10$ μm, $D_g = 0.2$ cm^2/s, $v = 250$ m/s, $\gamma = 0.03$.

Several approximations have been previously used in such models, but all have significant shortcomings. Early models appreciated the intermittent nature of clouds and alternated cloudy and cloud-free conditions in each grid cell in proportion to the time that air resides within cloud (Lelieveld & Crutzen, 1990, 1991; Liang & Jacob, 1997). However, this approach is complex to implement, computationally slow, and we are not aware of current 3-D models that use it. Instead, many chemical transport models apply equation (1) using a grid-average surface area density, $f_c A$, where A is the surface area density within cloud and f_c is the cloud fraction of the grid cell (Huijnen et al., 2014; Jacob et al., 2004; Parrella et al., 2012; Williams et al., 2009). In this "thin-cloud approximation," the resulting characteristic loss time is $(f_c k_i)^{-1}$, which is 20–60 s for N$_2$O$_5$ and cloud fractions in the range $0.1 < f_c < 0.5$. This loss rate is much too fast (Figure 1; Müller, 2014) because it is equivalent to spreading cloud water throughout the grid cell or assuming that cloudy and cloud-free air are continuously well mixed, making all gas in the grid cell susceptible to cloud uptake. Another approach is to partition the grid cell into portions that are within cloud and subject to uptake and another portion that is not (Tost et al., 2006). If this "cloud partitioning method" is applied at the start of each model time step, it implicitly assumes that mixing between cloudy and clear air portions of the grid cell happens with the same timescale as the model time step. If the time step is changed, as commonly happens when changing model resolution, then the entrainment and gas-aqueous exchange rates are altered, which is unphysical (Figure 1). Furthermore, for fast reactions, the numerical error actually rises as the time step is reduced, which violates expectations for numerical convergence.

We derive a more realistic treatment of reactive chemical uptake in partly cloudy conditions for use in global and regional atmospheric models. In this approach, which we call "entrainment-limited uptake," the gas concentration in the cloudy part of the grid cell, c_i, is depleted by heterogeneous surface or multiphase reactions at rate $k_i c_i$, where k_i is given by equation (1), and by detrainment to clear air at rate $k_c c_i$, where $\tau_c = 1/k_c$ is the residence time of air in cloud. The in-cloud concentration is also replenished by entrainment from clear air. As shown in the supporting information, the mass balance equations imply that gas is consumed from a partly cloudy grid cell at the rate

$$J = kc, \quad k = k_i \left(\frac{x}{1+x} \right), \tag{2}$$

where c is the usual grid cell concentration, which averages over cloudy and cloud-free regions. The term $x/(1+x)$ is the fraction of gas in the grid cell that is within cloud, and x is related to cloud properties and chemical rates by

$$x = \frac{1}{2}(f' - k' - 1) + \frac{1}{2}\left(1 + k'^2 + f'^2 + 2k' + 2f' - 2k'f'\right)^{1/2}, \quad k' \equiv \frac{k_i}{k_c}, f' \equiv \frac{f_c}{1-f_c}. \tag{3}$$

The supporting information provides a detailed derivation of these equations. The loss rate thus depends on the ratio of reactive uptake versus detrainment rates (k_i/k_c) as well as the cloud fraction (f_c). If meteorological and chemical data can provide f_c, k_c, and k_i, then numerical models can easily calculate k, but the controls on heterogeneous reaction rates are more apparent from the approximate solution

$$k \approx \widetilde{k} = \left(\frac{1}{f'k_c} + \frac{1}{f_c k_i} \right)^{-1} = \left(\frac{1-f_c}{f_c k_c} + \frac{r}{f_c A D_g} + \frac{4}{f_c A v \gamma} \right)^{-1}. \tag{4}$$

Within a cloud or aerosol, equation (1) shows that uptake is limited by gas phase diffusion (D_g term) and reactive uptake (γ term) acting in series. On scales larger than a single cloud, equation (4) shows that entrainment (k_c term) also limits uptake in series with the two in-cloud processes, so $k \leq k_i$. Under

completely cloudy conditions, the entrainment term vanishes and equation (4) reduces to equation (1) (i.e., $k = k_i$ when $f_c = 1$), meaning that our entrainment-limited uptake is a generalization of the Schwartz (1986) equation for partly cloudy conditions.

Scale analysis of equation (4) highlights the importance of entrainment for limiting the loss of N_2O_5, and other soluble compounds, in clouds. While the timescale for N_2O_5 loss inside a cloud is $k_i^{-1} \approx 10$ s, as we showed above, the characteristic time for loss in a partly cloudy region ($f_c = 0.1 - 0.5, \tau_c = 3,600$ s) is $k^{-1} = 1$–10 hr. For N_2O_5, the characteristic time is effectively determined by entrainment alone since $(f'k_c)^{-1}$ is 2–3 orders of magnitude larger than $(f_c k_i)^{-1}$. However, the in-cloud chemistry influences the loss rate for high cloud fractions ($f_c \gtrsim 0.95$), low uptake coefficients ($\gamma \lesssim 10^{-3}$), or very low surface area density ($A \lesssim 0.001$ cm^2/cm^3). In the limit of $k_i/k_c \ll 1$, meaning that in-cloud reactions are much slower than entrainment mixing, then $k \approx f_c k_i$, which is the thin-cloud approximation. Thus, the thin-cloud approximation is reasonable for reactions with an in-cloud characteristic time, k_i^{-1}, longer than about 10 hr (corresponding to $\gamma \lesssim 10^{-6}$).

Figure 1 illustrates the loss of N_2O_5 simulated with entrainment-limited uptake in comparison to the thin-cloud and cloud partitioning methods, all using the same assumptions about cloud properties. In the thin-cloud approximation, all N_2O_5 is lost within minutes. The cloud partitioning method simulates slower N_2O_5 loss, but loss rate is inversely proportional to the time step of the model, growing faster as the step size decreases. Only the entrainment-limited approach simulates slow, steady loss over hours, and the results are practically indistinguishable between the exact (equations (2) and (3)) and approximate (equation (4)) expressions. Because the entrainment-limited uptake is encapsulated in a first-order loss coefficient, it has very minimal computational cost while producing much greater realism compared to the other approaches.

3. Model Description

We assess the impact of clouds on N_2O_5 hydrolysis and tropospheric chemistry using the GEOS-Chem global chemical transport model (version 11-01, www.geos-chem.org). Simulations here use the tropospheric chemistry mechanism (Parrella et al., 2012). MERRA-2 (Modern-Era Retrospective Reanalysis for Research and Applications, Version 2) reanalysis meteorology (Gelaro et al., 2017) drives transport and provides cloud properties, which we resolve at $4° \times 5°$ and 47 vertical layers. Prior work has found that the sensitivity of global chemical responses to perturbations are generally consistent across model resolutions (Holmes et al., 2013). Emissions follow the model defaults. For NO_x, this includes the EDGAR global fossil fuel inventory (version 4.2; EC-JRC, 2011) and Yevich and Logan (2003) biofuel inventory, which are replaced by regional inventories where they are available (NEI2011v1 in United States: United States Environmental Protection Agency, 2015; Travis et al., 2016; BRAVO in Mexico: Kuhns et al., 2005; CAC in Canada: van Donkelaar et al., 2008; EMEP in Europe: European Monitoring and Evaluation Programme, 2014; and MIX in East Asia: Li et al., 2014). GFED4.1s provides biomass burning emissions (van der Werf et al., 2017). Soil and lightning NO_x emissions respond to the model's meteorology (Hudman et al., 2012; Murray et al., 2012) and include a bug fix for lightning (Lee Murray, personal communication, 9 August 2018).

The model previously included heterogeneous NO_x chemistry on aerosol surfaces (Evans & Jacob, 2005). We update the reactive uptake coefficients for consistency with recent literature (Table S1; Ammann et al., 2013; Atkinson et al., 2016; Bertram & Thornton, 2009; Bröske et al., 2003; Burkholder et al., 2015; Crowley, Ammann, et al., 2010; Escorcia et al., 2010; Fenter & Rossi, 1997; Ryder et al., 2015; Tan et al., 2016). In particular, NO_3 uptake on organic aerosol is slower (Atkinson et al., 2016) and N_2O_5 reactions on $SO_4^{2-} : NO_3^-$: NH_4^+ aerosol now depend on the H_2O and NO_3^- concentrations in aerosol (Bertram & Thornton, 2009; Shah et al., 2018). Past model versions assumed that the product of N_2O_5 uptake on all surfaces is entirely HNO_3. This is reasonable for clouds, but laboratory and field studies have demonstrated that aerosol uptake can produce $ClNO_2$, which escapes to the gas phase and recycles NO_x. The yield of $ClNO_2$ rises with the chloride content of the aerosol and reaches 1 for the concentrations found in sea salt aerosol (Behnke et al., 1997; Bertram & Thornton, 2009), so we adopt this yield for sea salt. For other aerosols in our simulations, the product remains HNO_3 because GEOS-Chem does not track the chloride content of nonsea salt aerosol. The simulated aerosol burden and optical depth, which are indicators of aerosol surface area, are consistent

with other recent global models (Myhre et al., 2013). As recommended by Atkinson et al. (2015), the model does not include homogeneous, gas phase hydrolysis of N_2O_5: $N_2O_5(g)+H_2O(g) \rightarrow 2HNO_3(g)$. Other models are sensitive to this reaction (Emmerson & Evans, 2009; Williams et al., 2009), however, so we assess its impact in a sensitivity simulation using an upper limit for the rate constant ($<1 \times 10^{-22}$ cm^3 molecule^{-1} s^{-1}; Atkinson et al., 2015).

We add uptake of N_2O_5, NO_3, and NO_2 on cloud water and cloud ice to the model using the entrainment-limited approach derived in section 2 (equations (2) and (3)) and recent assessments of reactive uptake coefficients (Table S1; Ammann et al., 2013; Burkholder et al., 2015; Crowley, Ammann, et al., 2010). The surface area of liquid water clouds, which is needed for equation (1), is derived from the MERRA-2 liquid water content using $A = 3L/\rho r$, where r is the effective radius and $\rho = 1,000$ kg/m^3 is the density of liquid water. We assume $r = 10$ μm for marine clouds and $r = 6$ μm for continental clouds. For ice clouds, we use the empirical, temperature-dependent effective radius, $r(T)$, reported by Heymsfield et al. (2014, their equation 9e). Bearing in mind that ice surface area is about 9 times larger than the cross-sectional area (Schmitt & Heymsfield, 2005), or 2.25 times the surface area of a sphere with the same effective radius, the ice surface area density is $A = 6.75I/\rho_{ice}r(T)$, where I is the MERRA-2 ice water content and $\rho_{ice} = 910$ kg/m^3 is the density of ice. When compared to satellite observations, MERRA-2 cloud properties reproduce the zonal mean and frequency distributions of optical depth and radiative effects within 30% (Bosilovich et al., 2015; Hongyu Liu, personal communication, 16 October 2018). Uncertainties in the cloud surface area and uptake coefficient have little effect on the results here because N_2O_5 and NO_3 uptake are primarily limited by entrainment and NO_2 uptake is very small. The residence time of air in clouds, which is used in the entrainment-limited uptake equations, varies by cloud type and weather conditions. MERRA-2, however, like many other meteorological reanalyses, provides only total cloud fraction, with no information about cloud types. In this work, we use $\tau_c = 1$ hr for the cloud residence time based on mean values for stratus and stratocumulus clouds (Feingold et al., 1998, 2013; Kogan, 2004; Stevens et al., 1996), which comprise a large fraction of global cloud cover (Lelieveld et al., 1989; Pruppacher & Jaenicke, 1995). Future work is needed to prescribe spatial and temporal variation in the cloud residence time from global reanalysis data.

The effects of heterogeneous reactions on NO_x, O_3, and OH chemistry are assessed in four simulations. The control simulation includes uptake on aerosols and clouds, as described above, and is our best representation of this heterogeneous chemistry. Three sensitivity tests neglect uptake on clouds, aerosols, or both. An additional sensitivity test includes homogeneous hydrolysis of N_2O_5. All simulations begin with 6 months of spin-up, and then results for 2015 are analyzed.

4. Impact of Cloud Heterogeneous Chemistry

Figure 2 shows the contributions of reaction pathways to NO_x loss by latitude in the model. Uptake of N_2O_5, NO_3, and NO_2 in clouds, the innovation in this work, is far from negligible, as suggested in past literature. Clouds provide 25% of NO_x loss at high latitudes and 1%–5% at low latitudes. In the Northern Hemisphere, most of this loss occurs in liquid water clouds because NO_x concentrations are highest at low altitudes due to surface emissions. In the Southern Hemisphere, NO_x is more evenly distributed vertically, so ice clouds provide most of the uptake. Aerosol uptake provides up to 30% of simulated NO_x loss in midlatitudes of the Northern Hemisphere, and homogeneous gas phase reactions provide the majority of NO_x loss at all latitudes. When integrated over just the lowest 2 km, aerosol uptake in our model rises to 50% of NO_x loss in northern midlatitudes, which is similar to results from field studies focused on this region (Aldener et al., 2006; Jaegle et al., 2018; Wagner et al., 2013).

Seasonally, heterogeneous NO_x loss on aerosols and liquid water clouds is greatest in winter, particularly in the northern extratropics (Figure 2b). This occurs for both aerosols and liquid water clouds. For loss on aerosols, the main driver of this seasonal cycle is the rise in N_2O_5 concentrations in winter due to its thermal stability at cold temperatures (Dentener & Crutzen, 1993; Platt et al., 1981). In our simulations, the mean N_2O_5 loss frequency on aerosols, which does not depend on N_2O_5 concentration, is nearly constant throughout the year in the northern extratropics (Figure 2c). Loss of N_2O_5 on liquid water clouds has a stronger seasonal cycle than loss on aerosols, meaning that the loss frequency is greater in winter than summer. This
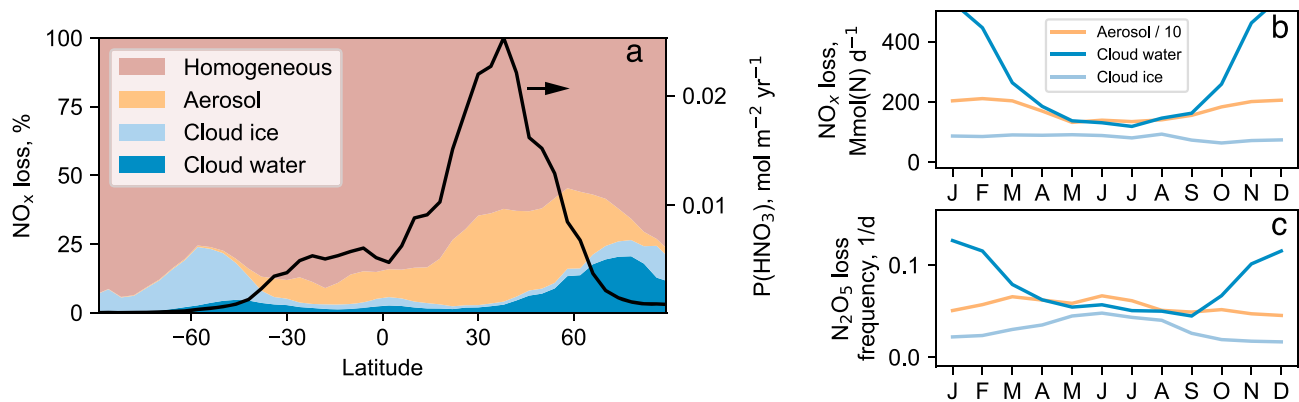
Figure 2. Chemical pathways for NO_x conversion to HNO_3 (a) in the zonal and annual mean, with black line showing HNO_3 production (right vertical axis), (b) by month in the northern hemisphere extratropics (30°N–90°N), and (c) N_2O_5 loss frequency in the northern extratropics.

happens because cloud coverage increases in winter, particularly in the Northern Hemisphere (Stubenrauch et al., 2006). The uptake coefficient ($\gamma_{N_2O_5}$) on liquid water also increases at cold temperatures (Burkholder et al., 2015), but this effect has little influence on the seasonal cycle because gas phase diffusion and cloud entrainment impose greater limits on uptake rate. The seasonal cycle of N_2O_5 uptake on ice clouds in the northern extratropics differs from uptake on liquid water clouds. In our simulations, ice clouds take up N_2O_5 more effectively in summer than winter (Figure 2c), despite the lesser extent of ice clouds in summer. The reason is that summertime convection transports NO_x to high altitudes where ice clouds persist. This effect offsets the seasonal cycle of N_2O_5 concentrations so that the overall loss of N_2O_5 on ice clouds is nearly constant year-round (Figure 2b).

Table 1 quantifies the global NO_x budget and the impact of neglecting heterogeneous reactions on tropospheric chemistry. Uptake on clouds is 5% of the global chemical NO_x sink (0.2 Tmol N/year) and aerosols remove another 27% (1.1 Tmol N/year). Most heterogeneous loss on both clouds and aerosols is from N_2O_5 uptake and, secondarily, from NO_3 uptake. NO_2 uptake is small on aerosols and negligible on clouds because of the very small reactive uptake coefficients (Table S1). Homogeneous reactions, primarily $NO_2 + OH \rightarrow HNO_3$ and $NO_3 + VOC \rightarrow HNO_3 +$ products, provide the remaining 68% of chemical loss. In addition to the chemical sinks, dry deposition of NO_2 and organic nitrates provides an additional sink for 0.3 Tmol N/year, which is similar to the cloud heterogeneous losses.

If the cloud heterogeneous reactions are neglected, the tropospheric NO_x burden in the model increases 0.7%, which results in a 2% increase in tropospheric O_3 and a 2% decrease in the CH_4 lifetime due to tropospheric OH. Neglecting heterogeneous aerosol reactions yields changes of a similar magnitude: 4% increase in NO_x, 3% increase in O_3, and 3% decrease in CH_4 lifetime. Thus, the impacts of aerosol and cloud heterogeneous chemistry on O_3 and CH_4 lifetime is similar, despite the fivefold greater NO_x loss on aerosols. The differences arise from the locations where NO_x is lost. Studies of aviation, ship, and industrial emissions show that marginal changes in NO_x abundance have the greatest effect on tropospheric O_3 in low-NO_x environments (Lin et al., 1988), particularly at low latitudes and high altitudes (Fry et al., 2012; Fuglestvedt et al., 2008; Holmes et al., 2014; Köhler et al., 2008, 2013). While aerosols remove NO_x mainly from the lower troposphere over industrial regions with high NO_x, clouds have a greater impact in remote, high-altitude, low-NO_x environments, which gives clouds a disproportionate impact on global O_3 and OH.

Table 1
Effect of Heterogeneous NO_x Chemistry on Tropospheric Composition and NO_x Loss

Simulation	Control	Cloud off[a]	Aerosol off[a]	Both off[a]
Aerosol reactions	Yes	Yes	No	No
Cloud reactions	Yes	No	Yes	No
NO_x	42.9 Gmol N	+0.7%	+3.8%	+8.9%
O_3	6.9 Tmol	+2.4%	+2.5%	+7.0%
OH	16.3 Mmol	+2.7%	+2.0%	+6.0%
τ_{CH_4+OH}	8.7 year	−1.9%	−3.4%	−6.9%
NO_x sinks, Tmol N/year				
Total P(HNO_3)	4.11	−0.8%	−2.4%	−5.7%
Homogeneous[b]	2.89	+3.2%	+21.4%	+33.0%
NO_2 + aerosol	0.04	−0.6%	—	—
NO_3 + aerosol	0.13	+2.9%	—	—
N_2O_5 + aerosol	0.80	+10.8%	—	—
NO_2 + cloud	0.00	—	+24.1%	—
NO_3 + cloud	0.02	—	+73.9%	—
N_2O_5 + cloud	0.19	—	+131%	—
Deposition[c]	0.29	+0.7%	+27.1%	+49.1%

[a]Percent changes are (Experimental − Control)/(Control) × 100%. [b]$NO_2 + OH \rightarrow HNO_3$ and $NO_3 + VOC \rightarrow HNO_3 +$ products. Homogeneous hydrolysis of N_2O_5 could provide an additional 0.1 Tmol N/year. [c]Dry and wet deposition of NO_2, N_2O_5, and organic nitrates. Of these, dry deposition of NO_2 and organic nitrates are each roughly half and others are much smaller.

Cloud uptake modestly shifts the simulated HNO_3 deposition, which is relevant for acid rain and nutrient loading (Figure S1). Although absolute changes in deposition are small, the overall effect of clouds is to increase HNO_3 deposition in the middle and high latitudes by about 2%, particularly in the storm tracks, where clouds are most prevalent. There is a compensating 2% decrease of HNO_3 deposition in the marine subtropical subsidence zones, due to the reduced HNO_3 production from $OH + NO_2$. Over the tropical continents, which have both clouds and high OH levels, the two effects compete, but the model suggests that adding the cloud uptake increases HNO_3 deposition by 1% in these regions.

Our results suggest that tropospheric NO_x, O_3, and OH levels are much less sensitive to heterogeneous aerosol chemistry than previous model studies suggested. For example, Macintyre and Evans (2010) reported that omitting N_2O_5 uptake on aerosols raised tropospheric NO_x by about 15% and O_3 and OH by 5%, which is 2–3 times the effect that we report (Table 1 and above). Earlier studies reported even greater sensitivity, but subsequent studies found that their $\gamma_{N_2O_5}$ values on aerosol were too high (Dentener & Crutzen, 1993; Tie et al., 2001). Part of the explanation is that we treat the product of N_2O_5 uptake to sea salt aerosol as $HNO_3 + ClNO_2$, rather than $2HNO_3$, as in past models. That change reduces the NO_x sink from aerosol heterogeneous reactions by 15% since sea salt accounts for one third of global N_2O_5 loss on aerosol in our model. However, the major reason for our lesser sensitivity is that clouds and aerosols compete for the same, limited supply of N_2O_5 and NO_3, so any changes in aerosol uptake are largely offset, or buffered, by opposing changes in cloud uptake. When aerosol uptake of NO_x is removed from the model, NO_x uptake on clouds increases 60%. This competition explains why the results of neglecting both cloud and aerosol heterogeneous reactions simultaneously are much greater than the sum of neglecting them individually (Table 1).

Although the addition of heterogeneous NO_x chemistry in clouds has significant impacts on tropospheric oxidant chemistry and budgets, discussed above, adding this chemistry has little meaningful effect on the model's comparison to most aircraft and sonde observations of NO_x and O_3. This is because the 1%–3% decreases in mean background NO_x and O_3 due to cloud chemistry are much smaller than the environmental variability or prior model biases for these gases (Jacob et al., 2003; Logan, 1999; Logan et al., 2012). Examples are shown in Figure S2. The mechanism could potentially be tested further with nighttime airborne measurements of N_2O_5 and NO_3 lifetimes (e.g., Brown et al., 2006, 2009) averaged over large, partly cloudy, low-aerosol regions. The chemistry of N_2O_5 uptake on water and ice is sufficiently well understood, however, that the reaction should be included in atmospheric models regardless of its benefit or detriment to observational comparisons. Nevertheless, this shift should slightly diminish the surface O_3 bias found in many models (Young et al., 2018) and push the model closer to the observationally constrained CH_4 lifetime (11.2 $\pm$ 1.3 year versus 8.7 year simulated; Prather et al., 2012). Considering that doubling the spatial resolution to $2° \times 2.5°$ increases the lifetime about 0.5 year (Holmes et al., 2013), a higher-resolution version of the present model using the same chemistry would likely be at the lower end of the uncertainty envelope.

Recent global model studies disagree on the relative importance of processes contributing to HNO_3 and nitrate production. Most have neglected N_2O_5 and NO_3 uptake in clouds (Alexander et al., 2009; Bauer, 2004; Hauglustaine et al., 2014; Xu & Penner, 2012), but one study suggested that this process provides 41% of HNO_3 production (Williams et al., 2009). That model used the thin-cloud approximation, however, which significantly overestimates N_2O_5 uptake, as we showed in section 2, so our estimate of 5% is likely more realistic. Heterogeneous reactions on aerosols are reported to provide 8%–41% of global HNO_3 production (Alexander et al., 2009; Bauer, 2004; Hauglustaine et al., 2014; Williams et al., 2009; Xu & Penner, 2012). Trends and variability in aerosol surface area will change the aerosol uptake rate, and these studies examined different years, but that is unlikely to account for the large range. However, the smallest estimate included reactions only on sulfate aerosol (Hauglustaine et al., 2014), and the largest assumed a very large uptake coefficient ($\gamma_{N_2O_5} = 0.1$; Xu & Penner, 2012). Neglecting those extremes, the literature suggests that aerosol uptake is 18%–35% of HNO_3 production. Our result of 27% falls in the middle of this range. Homogeneous hydrolysis of N_2O_5 is neglected in many models, because its rate and importance remain unclear (Alecu & Marshall, 2014; Atkinson et al., 2015; Brown & Stutz, 2012; Brown et al., 2009; Crowley, Schuster, et al., 2010), but the reaction has a meaningful impact on tropospheric O_3 when it is included in box models (Emmerson & Evans, 2009). Contrary to the box model results, tests in our global model using the upper limit rate from IUPAC (Atkinson et al., 2015) find that homogeneous hydrolysis supplies less than 2% of global HNO_3 production (0.1 Tmol N/year) and changes mean tropospheric O_3 and OH by under 0.5%

each. Another global model also reported a similar upper limit on HNO_3 production (<5%, 0.1 Tmol N/year; Williams et al., 2009), implying that the homogeneous hydrolysis rate for N_2O_5 is likely not a major source of uncertainty in tropospheric chemistry modeling.

5. Conclusions

While the global importance of heterogeneous NO_x chemistry on aerosol surfaces has been widely recognized for several decades (Dentener & Crutzen, 1993; Heikes & Thompson, 1983; Jacob, 2000), heterogeneous reactions in clouds have been thought to be minor or negligible. Our results, however, show that heterogeneous NO_x loss in clouds plays a significant role in the tropospheric NO_x cycle and meaningfully impacts tropospheric oxidants. Cloud uptake provides up to 25% of tropospheric NO_x loss at high latitudes and averages 5% globally. Homogeneous, gas phase hydrolysis of N_2O_5 is likely 2% or less of the tropospheric NO_x sink. Although aerosols take up more NO_x than clouds, neglecting either cloud or aerosol heterogeneous reactions in an atmospheric chemistry model has similar impacts on global tropospheric chemistry: raising the tropospheric O_3 burden by about 2% and reducing the CH_4 lifetime due to tropospheric OH by 2%. Moreover, accounting for NO_x uptake on clouds nearly halves the sensitivity of tropospheric oxidants to heterogeneous aerosol reactions, because both clouds and aerosols compete for the same NO_3 and N_2O_5.

The method of entrainment-limited uptake, which we developed here, has clear advantages over other approaches used to simulate cloud chemistry in atmospheric chemistry models. The method better represents cloud heterogeneous rates than the widely used thin cloud or cloud partitioning approaches while adding little or no computational burden to numerical chemical solvers. Future work to specify spatiotemporal variation in the residence time of air in clouds could further improve the method. The entrainment-limited equations are appropriate for any prognostic atmospheric chemistry model that does not resolve individual clouds, whether global or regional, and applicable to any reactive compound with irreversible surface or multiphase loss. Beyond NO_x cycling, which we examined here, the method may advance global modeling and understanding of other cloud chemical reactions, including HO_2 and formaldehyde uptake, photolysis, SO_2 oxidation, mercury reduction, and aerosol processing.

References

Aldener, M., Brown, S. S., Stark, H., Williams, E. J., Lerner, B. M., Kuster, W. C., et al. (2006). Reactivity and loss mechanisms of NO_3 and N_2O_5 in a polluted marine environment: Results from in situ measurements during New England Air Quality Study 2002. *Journal of Geophysical Research*, *111*, D23S73. https://doi.org/10.1029/2006JD007252

Alecu, I. M., & Marshall, P. (2014). Computational study of the thermochemistry of N_2O_5 and the kinetics of the reaction $N_2O_5 + H_2O \rightarrow 2$ HNO_3. *Journal of Physical Chemistry A*, *118*(48), 11,405–11,416. https://doi.org/10.1021/jp509301t

Alexander, B., Hastings, M. G., Allman, D. J., Dachs, J., Thornton, J. A., & Kunasek, S. A. (2009). Quantifying atmospheric nitrate formation pathways based on a global model of the oxygen isotopic composition (^{17}O) of atmospheric nitrate. *Atmospheric Chemistry and Physics*, *9*(14), 5043–5056. https://doi.org/10.5194/acp-9-5043-2009

Ammann, M., Cox, R. A., Crowley, J. N., Jenkin, M. E., Mellouki, A., Rossi, M. J., et al. (2013). Evaluated kinetic and photochemical data for atmospheric chemistry: Volume VI—Heterogeneous reactions with liquid substrates. *Atmospheric Chemistry and Physics*, *13*(16), 8045–8228. https://doi.org/10.5194/acp-13-8045-2013

Atkinson, R., Baulch, D. L., Cox, R. A., Crowley, J. N., Hampson, R. F., Hynes, R. G., et al. (2015). Data sheet NOx33. In IUPAC task group on atmospheric chemical kinetic data evaluation. Retrieved 20 February 2019 from http://iupac.pole-ether.fr

Atkinson, R., Baulch, D. L., Cox, R. A., Crowley, J. N., Hampson, R. F., Hynes, R. G., et al.(2016). Data sheet Het_Org1. In IUPAC task group on atmospheric chemical kinetic data evaluation. Retrieved 15 August 2018 from http://iupac.pole-ether.fr

Atkinson, R., Winer, A. M., & Pitts, J. N. Jr. (1986). Estimation of night-time N_2O_5 concentrations from ambient NO_2 and NO_3 radical concentrations and the role of N_2O_5 in night-time chemistry. *Atmospheric Environment*, *20*(2), 331–339. https://doi.org/10.1016/0004-6981(86)90035-1

Bauer, S. E. (2004). Global modeling of heterogeneous chemistry on mineral aerosol surfaces: Influence on tropospheric ozone chemistry and comparison to observations. *Journal of Geophysical Research*, *109*, D02304. https://doi.org/10.1029/2003JD003868

Behnke, W., George, C., Scheer, V., & Zetzsch, C. (1997). Production and decay of $ClNO_2$ from the reaction of gaseous N_2O_5 with NaCl solution: Bulk and aerosol experiments. *Journal of Geophysical Research*, *102*(D3), 3795–3804. https://doi.org/10.1029/96JD03057

Bertram, T. H., & Thornton, J. A. (2009). Toward a general parameterization of N_2O_5 reactivity on aqueous particles: The competing effects of particle liquid water, nitrate and chloride. *Atmospheric Chemistry and Physics*, *9*, 8351–8363.

Bosilovich, M. G., Akella, S., Coy, L., Cullather, R., Draper, C., Gelaro, R., et al. (2015). MERRA-2: Initial Evaluation of the Climate (R. D. Koster, Ed.) (Technical Report Series on Global Modeling and Data Assimilation, NASA/TM–2015-104606 Vol. *43*, pp. 1–145). Greenbelt: NASA Goddard Space Flight Center.

Bröske, R., Kleffmann, J., & Wiesen, P. (2003). Heterogeneous conversion of NO_2 on secondary organic aerosol surfaces: A possible source of nitrous acid (HONO) in the atmosphere? *Atmospheric Chemistry and Physics*, *3*(3), 469–474. https://doi.org/10.5194/acp-3-469-2003

Brown, S. S., Ryerson, T. B.,Wollny, A. G., Brock, C. A., Peltier, R., Sullivan, A. P., et al. (2006). Variability in nocturnal nitrogen oxide processing and its role in regional air quality. *Science*, *311*(5757), 67–70. https://doi.org/10.1126/science.1120120

Brown, S. S., Dubé, W. P., Fuchs, H., Ryerson, T. B., Wollny, A. G., Brock, C. A., et al. (2009). Reactive uptake coefficients for N_2O_5 determined from aircraft measurements during the Second Texas Air Quality Study: Comparison to current model parameterizations. *Journal of Geophysical Research*, *114*, DO0F10. https://doi.org/10.1029/2008JD011679

Brown, S. S., Dubé, W. P., Osthoff, H. D., Stutz, J., Ryerson, T. B., Wollny, A. G., et al. (2007). Vertical profiles in NO_3 and N_2O_5 measured from an aircraft: Results from the NOAA P-3 and surface platforms during the New England Air Quality Study 2004. *Journal of Geophysical Research*, *112*, D23304. https://doi.org/10.1029/2007JD008883

Brown, S. S., Dubé, W. P., Tham, Y. J., Zha, Q., Xue, L., Poon, S., et al. (2016). Nighttime chemistry at a high altitude site above Hong Kong. *Journal of Geophysical Research: Atmospheres*, *121*, 2457–2475. https://doi.org/10.1002/2015JD024566

Brown, S. S., Stark, H., Ryerson, T. B., Williams, E. J., Nicks, D. K. Jr., Trainer, M., et al. (2003). Nitrogen oxides in the nocturnal boundary layer: Simultaneous in situ measurements of NO_3, N_2O_5, NO_2, NO, and O_3. *Journal of Geophysical Research*, *108*(D9), 4299. https://doi.org/10.1029/2002JD002917

Brown, S. S., & Stutz, J. (2012). Nighttime radical observations and chemistry. *Chemical Society Reviews*, *41*(19), 6405–6447. https://doi.org/10.1039/c2cs35181a

Burkholder, J. B., Sander, S. P., Abbatt, J. P. D., Barker, J. R., Huie, R. E., Kolb, C. E., et al. (2015). *Chemical Kinetics and Photochemical Data for use in Atmospheric Studies*, (Vol. 15). Pasadena: Jet Propulsion Laboratory.

Chang, W. L., Bhave, P. V., Brown, S. S., Riemer, N., Stutz, J., & Dabdub, D. (2011). Heterogeneous atmospheric chemistry, ambient measurements, and model calculations of N_2O_5: A review. *Aerosol Science and Technology*, *45*(6), 665–695. https://doi.org/10.1080/02786826.2010.551672

Crowley, J. N., Ammann, M., Cox, R. A., Hynes, R. G., Jenkin, M. E., Mellouki, A., et al. (2010). Evaluated kinetic and photochemical data for atmospheric chemistry: Volume V—Heterogeneous reactions on solid substrates. *Atmospheric Chemistry and Physics*, *10*(18), 9059–9223. https://doi.org/10.5194/acp-10-9059-2010

Crowley, J. N., Schuster, G., Pouvesle, N., Parchatka, U., Fischer, H., Bonn, B., et al. (2010). Nocturnal nitrogen oxides at a rural mountain-site in south-western Germany. *Atmospheric Chemistry and Physics*, *10*(6), 2795–2812. https://doi.org/10.5194/acp-10-2795-2010

Dentener, F. J., & Crutzen, P. J. (1993). Reaction of N_2O_5 on tropospheric aerosols: impact on the global distributions of NO_x, O_3, and OH. *Journal of Geophysical Research*, *98*(D4), 7149–7163. https://doi.org/10.1029/92JD02979

EC-JRC: European Commission Joint Research Centre, Netherlands Environmental Assessment Agency. (2011). Emission Database for Global Atmospheric Research (EDGAR) version 4.2. https://doi.org/10.2904/EDGARv4.2

Emmerson, K. M., & Evans, M. J. (2009). Comparison of tropospheric gas-phase chemistryschemes for use within global models. *Atmospheric Chemistry and Physics*, *9*(5), 1831–1845. https://doi.org/10.5194/acp-9-1831-2009

Escorcia, E. N., Sjostedt, S. J., & Abbatt, J. P. D. (2010). Kinetics of N_2O_5 hydrolysis on secondary organic aerosol and mixed ammonium bisulfate−secondary organic aerosol particles. *Journal of Physical Chemistry A*, *114*(50), 13,113–13,121. https://doi.org/10.1021/jp107721v

European Monitoring and Evaluation Programme. (2014). Inventory review 2014. European Environment Agency and Centre on Emission Inventories and Projections. Retrieved from http://www.ceip.at/fileadmin/inhalte/emep/pdf/2014/DP-143_InventoryReport_2014_forWeb.pdf

Evans, M. J., & Jacob, D. J. (2005). Impact of new laboratory studies of N_2O_5 hydrolysis on global model budgets of tropospheric nitrogen oxides, ozone, and OH. *Geophysical Research Letters*, *32*, L09813. https://doi.org/10.1029/2005GL022469

Feingold, G., Kreidenweis, S. M., & Zhang, Y. (1998). Stratocumulus processing of gases and cloud condensation nuclei: 1. Trajectory ensemble model. *Journal of Geophysical Research*, *103*(D16), 19,527–19,542. https://doi.org/10.1029/98JD01750

Feingold, G., McComiskey, A., Rosenfeld, D., & Sorooshian, A. (2013). On the relationship between cloud contact time and precipitation susceptibility to aerosol. *Journal of Geophysical Research: Atmospheres*, *118*, 10,544–10,554. https://doi.org/10.1002/jgrd.50819

Fenter, F. F., & Rossi, M. J. (1997). Heterogeneous reaction of NO_3 with ice and sulfuric acid solutions: Upper limits for the uptake coefficients. *Journal of Physical Chemistry A*, *101*(22), 4110–4113. https://doi.org/10.1021/jp970162q

Finlayson-Pitts, B. J., Ezell, M. J., & Pitts, J. N. Jr. (1989). Formation of chemically active chlorine compounds by reactions of atmospheric NaCl particles with gaseous N_2O_5 and $ClONO_2$. *Nature*, *337*(6204), 241–244. https://doi.org/10.1038/337241a0

Folberth, G. A., Hauglustaine, D. A., Lathiére, J., & Brocheton, F. (2006). Interactive chemistry in the Laboratoire de Météorologie Dynamique general circulation model: Model description and impact analysis of biogenic hydrocarbons on tropospheric chemistry. *Atmospheric Chemistry and Physics*, *6*(8), 2273–2319. https://doi.org/10.5194/acp-6-2273-2006

Fry, M. M., Naik, V., West, J. J., Schwarzkopf, M. D., Fiore, A. M., Collins, W. J., et al. (2012). The influence of ozone precursor emissions from four world regions on tropospheric composition and radiative climate forcing. *Journal of Geophysical Research*, *117*, D07306. https://doi.org/10.1029/2011JD017134

Fuchs, N. A., & Sutugin, A. G. (1971). High-dispersed aerosols. In G. M. Hidy, & J. R. Brock (Eds.), *Topics in Current Aerosol Research*, (pp. 1–60). New York: Pergamon Press.

Fuglestvedt, J., Berntsen, T., Myhre, G., Rypdal, K., & Skeie, R. B. (2008). Climateforcing from the transport sectors. *Proceedings of the National Academy of Sciences*, *105*(2), 454–458. https://doi.org/10.1073/pnas.0702958104

Gelaro, R., McCarty, W., Suarez, M. J., Todling, R., Molod, A., Takacs, L., et al. (2017). The Modern-Era Retrospective Analysis for Research and Applications, Version 2 (MERRA-2). *Journal of Climate*, *30*(14), 5419–5454. https://doi.org/10.1175/JCLI-D-16-0758.1

Hauglustaine, D. A., Balkanski, Y., & Schulz, M. (2014). A global model simulation of present and future nitrate aerosols and their direct radiative forcing of climate. *Atmospheric Chemistry and Physics*, *14*(20), 11,031–11,063. https://doi.org/10.5194/acp-14-11031-2014

Heald, C. L., Ridley, D. A., Kroll, J. H., Barrett, S. R. H., Cady-Pereira, K. E., Alvarado, M. J., & Holmes, C. D. (2014). Contrasting the direct radiative effect and direct radiative forcing of aerosols. *Atmospheric Chemistry and Physics*, *14*(11), 5513–5527. https://doi.org/10.5194/acp-14-5513-2014

Heikes, B. G., & Thompson, A. M. (1983). Effects of heterogeneous processes on NO_3, HONO, and HNO_3 chemistry in the troposphere. *Journal of Geophysical Research*, *88*(C15), 10,883–10,895. https://doi.org/10.1029/JC088iC15p10883

Heymsfield, A., Winker, D., Avery, M., Vaughan, M., Diskin, G., Deng, M., et al. (2014). Relationships between ice water content and volume extinction coefficient from in situ observations for temperatures from 0° to –86 °C: Implications for spaceborne lidar retrievals. *Journal of Applied Meteorology and Climatology*, *53*(2), 479–505. https://doi.org/10.1175/JAMC-D-13-087.1

Holmes, C. D., Prather, M. J., Søvde, O. A., & Myhre, G. (2013). Future methane, hydroxyl, and their uncertainties: Key climate and emission parameters for future predictions. *Atmospheric Chemistry and Physics*, *13*(1), 285–302. https://doi.org/10.5194/acp-13-285-2013

Holmes, C. D., Prather, M. J., & Vinken, G. C. M. (2014). The climate impact of ship NO_x emissions: an improved estimate accounting for plume chemistry. *Atmospheric Chemistry and Physics*, *14*, 6801–6812. https://doi.org/10.5194/acp-14-6801-2014

Hudman, R. C., Moore, N. E., Mebust, A. K., Martin, R. V., Russell, A. R., Valin, L. C., & Cohen, R. C. (2012). Steps towards a mechanistic model of global soil nitric oxide emissions: implementation and space based-constraints. *Atmospheric Chemistry and Physics*, *12*(16), 7779–7795. https://doi.org/10.5194/acp-12-7779-2012

Huijnen, V., Williams, J. E., & Flemming, J. (2014). Modeling global impacts of heterogeneous loss of HO$_2$ on cloud droplets, ice particles and aerosols. *Atmospheric Chemistry and Physics Discussions*, *14*(6), 8575–8632. https://doi.org/10.5194/acpd-14-8575-2014

Jacob, D. J. (2000). Heterogeneous chemistry and tropospheric ozone. *Atmospheric Environment*, *34*(12-14), 2131–2159.

Jacob, D. J., Crawford, J. H., Kleb, M. M., Connors, V. S., Bendura, R. J., Raper, J. L., et al. (2003). Transport and Chemical Evolution over the Pacific (TRACE-P) aircraft mission: Design, execution, and first results. *Journal of Geophysical Research*, *108*(D20), 9000. https://doi.org/10.1029/2002JD003276

Jacob, D. J., Field, B., & Chin, M. (2004). Natural and transboundary pollution influences on sulfate-nitrate-ammonium aerosols in the United States: Implications for policy. *Journal of Geophysical Research*, *109*, D15204. https://doi.org/10.1029/2003JD004473

Jaegle, L., Shah, V., Thornton, J. A., Lopez-Hilfiker, F. D., Lee, B. H., McDuffie, E. E., et al. (2018). Nitrogen oxides emissions, chemistry, deposition, and export over the northeast United States during the WINTER aircraft campaign. *Journal of Geophysical Research: Atmospheres*, *123*, 12,368–12,393. https://doi.org/10.1029/2018JD029133

Kogan, Y. L. (2004). Large-eddy simulation of air parcels in stratocumulus clouds: Time scales and spatial variability. *Journal of the Atmospheric Sciences*, *63*, 952–967. https://doi.org/10.1175/JAS3665.1

Köhler, M. O., Rädel, G., Dessens, O., Shine, K. P., Rogers, H. L., Wild, O., & Pyle, J. A. (2008). Impact of perturbations to nitrogen oxide emissions from global aviation. *Journal of Geophysical Research*, *113*, D11305. https://doi.org/10.1029/2007JD009140

Köhler, M. O., Rädel, G., Shine, K. P., Rogers, H. L., & Pyle, J. A. (2013). Latitudinal variation of the effect of aviation NOx emissions on atmospheric ozone and methane and related climate metrics. *Atmospheric Environment*, *63*, 1–9. https://doi.org/10.1016/j.atmosenv.2012.09.013

Kuhns, H., Knipping, E. M., & Vukovich, J. M. (2005). Development of a United States–Mexico Emissions Inventory for the Big Bend Regional Aerosol and Visibility Observational (BRAVO) study. *Journal of the Air & Waste Management Association*, *55*(5), 677–692. https://doi.org/10.1080/10473289.2005.10464648

Lelieveld, J., & Crutzen, P. J. (1990). Influences of cloud photochemical processes on tropospheric ozone. *Nature*, *343*, 227–233. https://doi.org/10.1038/343227a0

Lelieveld, J., & Crutzen, P. J. (1991). The role of clouds in tropospheric photochemistry. *Journal of Atmospheric Chemistry*, *12*, 229–267. https://doi.org/10.1007/BF00048075

Lelieveld, J., Crutzen, P. J., & Rodhe, H. (1989). *Zonal Average Cloud Characteristics for Global Atmospheric Chemistry Modelling*, GLOMAC-report UDC 551.510.4, CM-74 (pp. 1–54). Stockholm, Sweeden: International Meteorological Institute in Stockholm.

Li, M., Zhang, Q., Streets, D. G., He, K. B., Cheng, Y. F., Emmons, L. K., et al. (2014). Mapping Asian anthropogenic emissions of non-methane volatile organic compounds to multiple chemical mechanisms. *Atmospheric Chemistry and Physics*, *14*(11), 5617–5638. https://doi.org/10.5194/acp-14-5617-2014

Liang, J., & Jacob, D. J. (1997). Effect of aqueous phase cloud chemistry on tropospheric ozone. *Journal of Geophysical Research*, *1-2*(D5), 5993–6001. https://doi.org/10.1029/96JD02957

Liao, H., Adams, P. J., Chung, S. H., Seinfeld, J. H., Mickley, L., & Jacob, D. (2003). Interactions between tropospheric chemistry and aerosols in a unified general circulation model. *Journal of Geophysical Research*, *108*(D1), 4001. https://doi.org/10.1029/2001JD001260

Lin, X., Trainer, M., & Liu, S. C. (1988). On the nonlinearity of the tropospheric ozone production. *Journal of Geophysical Research*, *93*(D12), 15,879–15,888. https://doi.org/10.1029/JD093iD12p15879

Logan, J. A. (1983). Nitrogen oxides in the troposphere: Global and regional budgets. *Journal of Geophysical Research*, *88*(C15), 10,785–10,807. https://doi.org/10.1029/JC088iC15p10785

Logan, J. A. (1999). An analysis of ozonesonde data for the troposphere: Recommendations for testing 3-D models and development of a gridded climatology for tropospheric ozone. *Journal of Geophysical Research*, *104*(D13), 16,115–16,149. https://doi.org/10.1029/1998JD100096

Logan, J. A., Staehelin, J., Megretskaia, I. A., Cammas, J. P., Thouret, V., Claude, H., et al. (2012). Changes in ozone over Europe: Analysis of ozone measurements from sondes, regular aircraft (MOZAIC) and alpine surface sites. *Journal of Geophysical Research*, *117*, D09301. https://doi.org/10.1029/2011JD016952

Macintyre, H. L., & Evans, M. J. (2010). Sensitivity of a global model to the uptake of N$_2$O$_5$ by tropospheric aerosol. *Atmospheric Chemistry and Physics*, *10*(15), 7409–7414. https://doi.org/10.5194/acp-10-7409-2010

McDuffie, E. E., Fibiger, D. L., Dubé, W. P., Lopez-Hilfiker, F., Lee, B. H., Thornton, J. A., et al. (2018). Heterogeneous N$_2$O$_5$ uptake during winter: aircraft measurements during the 2015 WINTER campaign and critical evaluation of current parameterizations. *Journal of Geophysical Research: Atmospheres*, *123*, 4345–4372. https://doi.org/10.1002/2018JD028336

Müller, J. F. (2014). Interactive comment on "Modeling global impacts of heterogeneous loss of HO$_2$ on cloud droplets, ice particles and aerosols". *Atmospheric Chemistry and Physics Discussions*, *14*, C982–C983.

Murray, L. T., Jacob, D. J., Logan, J. A., Hudman, R. C., & Koshak, W. J. (2012). Optimized regional and interannual variability of lightning in a global chemical transport model constrained by LIS/OTD satellite data. *Journal of Geophysical Research*, *117*, D20307. https://doi.org/10.1029/2012JD017934

Myhre, G., Samset, B. H., & Schulz, M. (2013). Radiative forcing of the direct aerosol effect from AeroCom Phase II simulations. *Atmospheric Chemistry and Physics*, *13*, 1853–1877. https://doi.org/10.5194/acp-13-1853-2013

Parrella, J. P., Jacob, D. J., Liang, Q., Zhang, Y., Mickley, L. J., Miller, B., et al. (2012). Tropospheric bromine chemistry: Implications for present and pre-industrial ozone and mercury. *Atmospheric Chemistry and Physics*, *12*(15), 6723–6740. https://doi.org/10.5194/acp-12-6723-2012

Platt, U., & Janssen, C. (1995). Observation and role of the free radicals NO$_3$, ClO, BrO and IO in the troposphere. *Faraday Discussions*, *100*, 175–198.

Platt, U., Perner, D., Schröder, J., Kessler, C., & Toennissen, A. (1981). The diurnal variation of NO$_3$. *Journal of Geophysical Research*, *86*(C12), 11,965–11,970. https://doi.org/10.1029/JC086iC12p11965

Podglajen, A., Plougonven, R., Hertzog, A., & Legras, B. (2016). A modelling case study of a large-scale cirrus in the tropical tropopause layer. *Atmospheric Chemistry and Physics*, *16*(6), 3881–3902. https://doi.org/10.5194/acp-16-3881-2016

Prather, M., Holmes, C., & Hsu, J. (2012). Reactive greenhouse gas scenarios: Systematic exploration of uncertainties and the role of atmospheric chemistry. *Geophysical Research Letters*, *39*, L09803. https://doi.org/10.1029/2012GL051440

Pruppacher, H. R., & Jaenicke, R. (1995). The processing of water vapor and aerosols by atmospheric clouds, a global estimate. *Atmospheric Research*, *38*(1-4), 283–295.

Ravishankara, A. R. (1997). Heterogeneous and multiphase chemistry in the troposphere. *Science*, *276*, 1058–1065. https://doi.org/10.1126/science.276.5315.1058

Ryder, O. S., Campbell, N. R., Morris, H., Forestieri, S., Ruppel, M. J., Cappa, C., et al. (2015). Role of organic coatings in regulating N_2O_5 reactive uptake to sea spray aerosol. *Journal of Physical Chemistry A*, *119*(48), 11,683–11,692. https://doi.org/10.1021/acs.jpca.5b08892

Sander, R. (1999). Modeling atmospheric chemistry: Interactions between gas-phase species and liquid cloud/aerosol particles. *Surveys in Geophysics*, *20*(1), 1–31.

Schmitt, C. G., & Heymsfield, A. J. (2005). Total surface area estimates for individual ice particles and particle populations. *Journal of Applied Meteorology*, *44*(4), 467–474. https://doi.org/10.1175/JAM2209.1

Schwartz, S. E. (1986). Mass-transport considerations pertinent to aqueous phase reactions of gases in liquid-water clouds. In W. Jaeschke (Ed.), *Chemistry of Multiphase Atmospheric Systems* (Vol. G6, pp. 415–471). Springer *NATO ASI Ser. G*. New York.

Shah, V., Jaeglé, L., Thornton, J. A., Lopez-Hilfiker, F. D., Lee, B. H., Schroder, J. C., et al. (2018). Chemical feedbacks weaken the wintertime response of particulate sulfate and nitrate to emissions reductions over the eastern United States. *Proceedings of the National Academy of Sciences of the United States of America*, *115*(32), 8110–8115. https://doi.org/10.1073/pnas.1803295115

Stevens, B., Feingold, G., Cotton, W. R., & Walko, R. L. (1996). Elements of the microphysical structure of numerically simulated nonprecipitating stratocumulus. *Journal of the Atmospheric Sciences*, *53*(7), 980–1006. https://doi.org/10.1175/1520-0469(1996)053<0980:EOTMSO>2.0.CO;2

Stubenrauch, C. J., Chedin, A., Rädel, G., Scott, N. A., & Serrar, S. (2006). Cloud properties and their seasonal and diurnal variability from TOVS Path-B. *Journal of Climate*, *19*(21), 5531–5553. https://doi.org/10.1175/JCLI3929.1

Tan, F., Tong, S., Jing, B., Hou, S., Liu, Q., Li, K., et al. (2016). Heterogeneous reactions of NO_2 with $CaCO_3$–$(NH_4)_2SO_4$ mixtures at different relative humidities. *Atmospheric Chemistry and Physics*, *16*(13), 8081–8093. https://doi.org/10.5194/acp-16-8081-2016

Thornton, J. A., & Abbatt, J. P. D. (2005). N_2O_5 reaction on submicron sea salt aerosol: kinetics, products, and the effect of surface active organics. *Journal of Physical Chemistry A*, *109*(44), 10,004–10,012. https://doi.org/10.1021/jp054183t

Thornton, J. A., Kercher, J. P., Riedel, T. P., Wagner, N. L., Cozic, J., Holloway, J. S., et al. (2010). A large atomic chlorine source inferred from mid-continental reactive nitrogen chemistry. *Nature*, *464*(7286), 271–274. https://doi.org/10.1038/nature08905

Tie, X., Brasseur, G., Emmons, L., Horowitz, L., & Kinnison, D. (2001). Effects of aerosols on tropospheric oxidants: A global model study. *Journal of Geophysical Research*, *106*(D19), 22,931–22,964. https://doi.org/10.1029/2001JD900206

Tost, H., Jockel, P., Kerkweg, A., Sander, R., & Lelieveld, J. (2006). Technical note: A new comprehensive SCAVenging submodel for global atmospheric chemistry modelling. *Atmospheric Chemistry and Physics*, *6*(3), 565–574. https://doi.org/10.5194/acp-6-565-2006

Travis, K. R., Jacob, D. J., Fisher, J. A., Kim, P. S., Marais, E. A., Zhu, L., et al. (2016). Why do models overestimate surface ozone in the Southeast United States? *Atmospheric Chemistry and Physics*, *16*(21), 13,561–13,577. https://doi.org/10.5194/acp-16-13561-2016

United States Environmental Protection Agency. (2015). Profile of the 2011 National Air Emissions Inventory. Retrieved from https://www.epa.gov/sites/production/files/2015-08/documents/lite_finalversion_ver10.pdf

van der Werf, G. R., Randerson, J. T., Giglio, L., van Leeuwen, T. T., Chen, Y., Rogers, B. M., et al. (2017). Global fire emissions estimates during 1997–2016. *Earth System Science Data*, *9*(15), 5785–5812. https://doi.org/10.5194/acp-9-5785-2009

van Donkelaar, A., Martin, R. V., Leaitch, W. R., Macdonald, A. M., Walker, T. W., Streets, D. G., et al. (2008). Analysis of aircraft and satellite measurements from the Intercontinental Chemical Transport Experiment (INTEX-B) to quantify long-range transport of East Asian sulfur to Canada. *Atmospheric Chemistry and Physics*, *8*(11), 2999–3014. https://doi.org/10.5194/acp-8-2999-2008

van Doren, J. M., Watson, L. R., Davidovits, P., Worsnop, D. R., Zahniser, M. S., & Kolb, C. E. (1990). Temperature dependence of the uptake coefficients of nitric acid, hydrochloric acid and nitrogen oxide (N_2O_5) by water droplets. *The Journal of Physical Chemistry*, *94*(8), 3265–3269. https://doi.org/10.1021/j100371a009

Wagner, N. L., Riedel, T. P., Young, C. J., Bahreini, R., Brock, C. A., Dubé, W. P., et al. (2013). N_2O_5 uptake coefficients and nocturnal NO_2 removal rates determined from ambient wintertime measurements. *Journal of Geophysical Research: Atmospheres*, *118*, 9331–9350. https://doi.org/10.1002/jgrd.50653

Williams, J. E., van Zadelhoff, G.-J., & Scheele, M. P. (2009). The effect of updating scavenging and conversion rates on cloud droplets and ice particles in the TM global chemistry transport model (TR-308, pp. 1–58). De Bilt: KNMI.

Xu, L., & Penner, J. E. (2012). Global simulations of nitrate and ammonium aerosols and their radiative effects. *Atmospheric Chemistry and Physics*, *12*(20), 9479–9504. https://doi.org/10.5194/acp-12-9479-2012

Yevich, R., & Logan, J. A. (2003). An assessment of biofuel use and burning of agricultural waste in the developing world. *Global Biogeochemical Cycles*, *17*(4), 1095. https://doi.org/10.1029/2002GB001952

Young, P. J., Naik, V., Fiore, A. M., Gaudel, A., Guo, J., Lin, M. Y., et al. (2018). Tropospheric Ozone Assessment Report: Assessment of global-scale model performance for global and regional ozone distributions, variability, and trends. *Elementa: Science of the Anthropocene*, *6*(10), 1–49. https://doi.org/10.1525/journal.elementa.265

The role of clouds in the tropospheric NOₓ cycle: a new modeling approach for cloud chemistry and its global implications

Christopher D. Holmes[1], Timothy H. Bertram[2], Kaitlyn L. Confer[1], Kelly A. Graham[1], Allison C. Ronan[1], Charles K. Wirks[1], Viral Shah[3]

1 Department of Earth, Ocean, and Atmospheric Science; Florida State University; Tallahassee, FL 32306, USA

2 Department of Chemistry; University of Wisconsin; Madison WI 53706, USA

3 Harvard John A. Paulson School of Engineering and Applied Sciences; Harvard University; Cambridge, MA 02138, USA

Corresponding author: Christopher D. Holmes (cdholmes@fsu.edu)

Contents of this file

Introduction

This supplement contains:

- A derivation of the entrainment-limited uptake equations;

- Additional figures showing simulated ozone and NOx, nitrate deposition, and the accuracy of the approximate entrainment-limited uptake equations;

- A table of reactive uptake coefficients used in this work.

Text S1. Derivation of entrainment-limited uptake in a partly cloudy environment

In a partly cloudy environment, the total mass m of a gas, such as N_2O_5, is the sum of mass inside cloud (m_i) and outside cloud (m_o): $m = m_i + m_o$. Within the cloud, the gas is susceptible to reactive uptake at a rate k_i determined by its reactivity (γ) and the surface area of condensed water according to Eq. 1. In-cloud air is also detrained to the cloud-free region at a rate k_c, where $\tau_c = 1/k_c$ is the residence time of air in cloud. Over the life cycle of the cloud, entrainment and detrainment of air must be equal, which implies that the mean rate for entrainment of cloud-free air is $k_c f_c (1 - f_c)^{-1}$, where f_c is the cloud fraction. The mass balance equations are, therefore,

$$\frac{dm_o}{dt} = -\frac{f_c}{1 - f_c} k_c m_o + k_c m_i \qquad \text{S1}$$

$$\frac{dm_i}{dt} = \frac{f_c}{1 - f_c} k_c m_o - k_c m_i - k_i m_i. \qquad \text{S2}$$

The system of Eqs. S1 and S2 can be solved numerically, but doing this within every grid cell of an atmospheric chemistry model would require doubling the chemical state variables and it is unnecessary, as we show here. Instead, recognize that the mass balance for the entire cell is

$$\frac{dm}{dt} = -k_i m_i. \qquad \text{S3}$$

We can eliminate m_i from this equation with the identity

$$m_i = m \left(\frac{m_i}{m_i + m_o}\right) = m \left(\frac{x}{1 + x}\right), \qquad \text{S4}$$

where $x \equiv m_i/m_o$ is the ratio of mass inside cloud to mass outside cloud. Given time, the system defined by Eqs. S1 and S2 will adjust to a steady decay in which x is constant while m_i, m_o, and m all decrease at the same fractional rate

$$\frac{1}{m_o} \frac{dm_o}{dt} = \frac{1}{m_i} \frac{dm_i}{dt}. \qquad \text{S5}$$

Combining S1, S2, and S5 yields the quadratic identity

$$x^2 + (1 + k' - f')x - f' = 0, \qquad k' \equiv \frac{k_i}{k_c}, f' \equiv \frac{f_c}{1 - f_c} \qquad \text{S6}$$

whose solution is

$$x = \frac{1}{2}(f' - k' - 1) + \frac{1}{2}\left(1 + k'^2 + f'^2 + 2k' + 2f' - 2k'f'\right)^{1/2}. \qquad \text{S7}$$

Combining Eqs. S3, S4, and S7, the mass balance equation for the total mass in a partly cloudy environment is

$$\frac{dm}{dt} = -km, \qquad k \equiv k_i \left(\frac{x}{1 + x}\right). \qquad \text{S8}$$

The mean concentration in the grid cell is $c = m/(MV)$, where M is the molecular mass and V is the grid cell volume, so the same k coefficient also describes the concentration loss. This exact expression for k is easily evaluated within a numerical model, but examining solutions under the limits $k_i/k_o \ll 1$ and $k_i/k_o \gg 1$ can provide a deeper understanding of the limiting processes.

In the limit $k_i \gg k_c$, meaning that the residence time of air in cloud is much longer than the characteristic timescale for in-cloud heterogeneous loss, we can neglect the detrainment terms ($k_c m_i$) in Eqs. S1 and S2. In that case, $x = f'k_c(k_i - f'k_c)^{-1}$ and the overall decay rate is $k = f'k_c$. In the opposite limit of $k_i \ll k_c$, meaning that in-cloud heterogenous loss is slow compared to cloud detrainment, the entrainment and detrainment mass fluxes in Eqs. S1 and S2 are approximately equal, which implies $x = f'$ and $k = f_c k_i$. An approximate solution that reproduces both limits and reasonably describes the intermediate behavior is

$$\tilde{k} = \left(\frac{1}{f_c k_i} + \frac{1}{f' k_c} \right)^{-1}. \qquad\qquad \text{S9}$$

Figure S3 evaluates the accuracy of the approximate $\tilde{k}$ against the exact solution k over a wide range of k_i/k_c and f_c. The error in $\tilde{k}$ is under 5% for $f_c \leq 0.2$ and never exceeds 50 %. For comparison, the median and mean cloud fractions in MERRA-2 are 0.06 and 0.2, respectively. The largest $\tilde{k}$ errors occur when mass is lost quickly anyway, so the maximum errors in simulated mass are only about 15%. The accuracy of $\tilde{k}$ relative to the exact k is similar to the widely used Schwartz (1986) equation for gas-aerosol mass transfer (Eq. 1), which also has errors that approach 40% under some conditions when compared to more accurate expressions (Fuchs & Sutugin, 1971; Sander, 1999). In both cases, the simpler solution may be acceptable when errors due to parameter uncertainty (e.g. γ, r, f_c, k_c) exceed the error of the approximation.
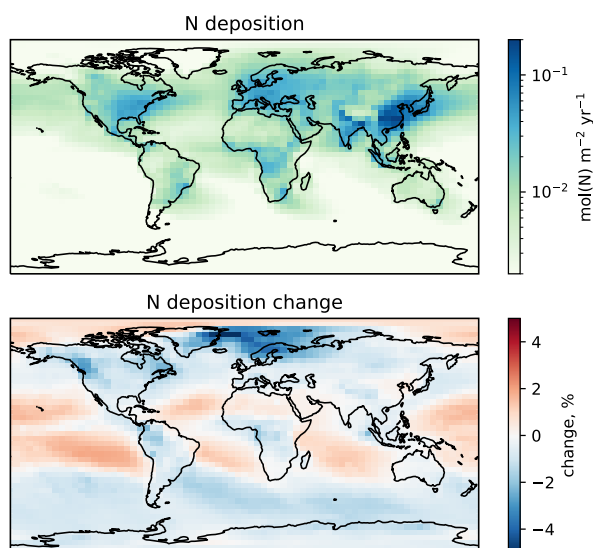

Figure S1. Inorganic nitrate deposition in the control simulation (top) and change due to neglecting cloud heterogeneous chemistry (bottom). Includes wet and dry deposition of gaseous HNO_3 and particulate NO_3^-. Change reported as (Cloud Off − Control)/Control × 100%.
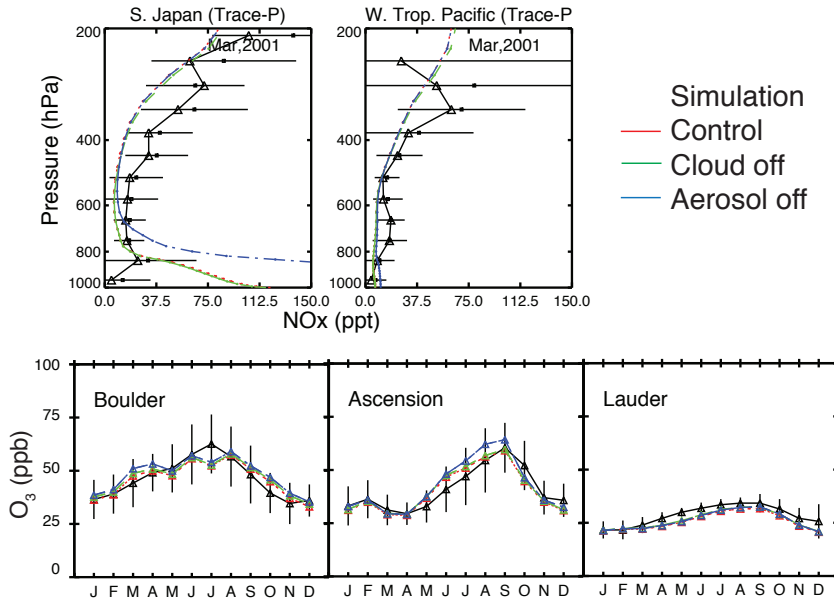
Figure S2. Simulated and observed NO$_x$ (top row) and O$_3$ (bottom row). NO$_x$ observations are from Trace-P aircraft (Jacob et al., 2003) and O$_3$ observations are from a sonde climatology at 800 hPa (Logan, 1999; Logan et al., 2012). Simulated values are monthly averages for 2015, not matched to the time of observations, in order to illustrate the modest effects of cloud and aerosol uptake relative to typical environmental variability.
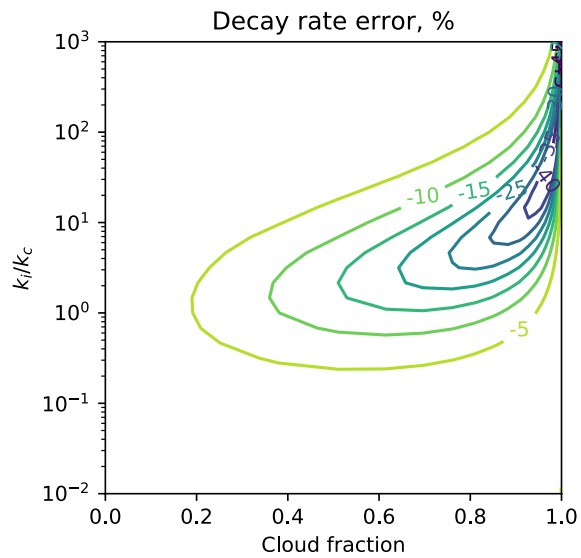

Figure S3. Error in approximate decay rate ($\widetilde{k}$, Eq. S9) expressed as percent difference from the exact numerical solution (k, Eq. S8). Maximum mass errors in 1 hour of simulation are about one-third of the decay rate errors.

Table S1. Reactive uptake coefficients (γ) used in this work for nitrogen gases on tropospheric cloud and aerosol surfaces.

Reaction, Surface	Uptake coefficient, γ[a]	Reference
NO_2 + surface → $0.5HNO_3$ + $0.5HONO$		
Cloud water	10^{-8}	(Ammann et al., 2013)[b]
Cloud ice	0	(Crowley et al., 2010)[c]
Dust	10^{-8}	(Crowley et al., 2010)
Black carbon	10^{-4}	(Burkholder et al., 2015)
Organic carbon	10^{-6}	(Bröske et al., 2003)[d]
Sea salt	10^{-8} (R < 40%) Interpolated (40% ≤ RH < 70%) 10^{-4} (RH ≥ 70%)	(Burkholder et al., 2015)
Sulfate	5×10^{-6}	(Tan et al., 2016)[e]
NO_3 + surface → HNO_3		
Cloud water	0.002	(Burkholder et al., 2015)
Cloud ice	0.001	(Burkholder et al., 2015)
Dust	0.01	(Crowley et al., 2010)
Black carbon	2×10^{-4} (RH < 50%) 1×10^{-3} (RH ≥ 50%)	(Burkholder et al., 2015)
Organic carbon	0.005	(Atkinson et al., 2016)[f]
Sea salt	0.05 (RH < 40%) Interpolated (40% ≤ RH < 70%) 0.002 (RH ≥ 70%)	(Ammann et al., 2013; Burkholder et al., 2015)[g]
Sulfate	0.001 (RH < 40%) 0.002 (RH ≥ 40%)	[h]
N_2O_5 + surface → $2HNO_3$		
Cloud water	$\left(\frac{0.03}{0.019}\right)\exp\left(-a+\frac{b}{T}-\frac{c}{T^2}\right)$, $a = 25.5265$, $b = 9283.76$ K, $c = 851801$ K^2	(Burkholder et al., 2015)[i]
Cloud ice	0.02	(Burkholder et al., 2015)
Dust	0.02	(Crowley et al., 2010)
Black carbon	0.005	(Evans & Jacob, 2005)[j]
Organic carbon	0.6×10^{-4} (RH < 30%) 1.5×10^{-4} (RH ≥ 30%)	(Escorcia et al., 2010)[k]
Sulfate	$f([NO_3^-], [H_2O])$	(Bertram & Thornton, 2009)[l]
N_2O_5 + surface → HNO_3 + $ClNO_2$		
Sea salt	0.005 (R < 40%) Interpolated (40% ≤ RH < 70%) 0.02 (RH ≥ 70%)	(Ammann et al., 2013; Thornton & Abbatt, 2005)[m]

[a] T is temperature (K). RH is relative humidity (%). Linear interpolation between RH endpoints is used for sea-salt aerosol.

[b] Coefficient depends on temperature, [NO_2], and solutes. Value adopted here is the recommendation for dilute water solutions at 273 K and 1 ppb NO_2. Cloud water is not expected to contain solutes at levels that would significantly raise the coefficient value.

[c] Upper limit is 10^{-4}, but this likely reflects a sticking coefficient.

[d] Midpoint of the reported range 10^{-7} to 10^{-5}.

[e] Value for $(NH_4)_2SO_4$.

[f] Value for pure alkane aerosol, which is similar to values for alcohols and carbonyls.

[g] Low RH value from Burkholder et al. (2015); high RH value from Ammann et al. (2013).

[h] No measurements on dry or wet sulfate-nitrate-ammonium aerosol are available. High RH value is for pure liquid water. Low RH value is an upper limit based on H_2SO_4 aerosol (Fenter & Rossi, 1997).

[i] Value is 0.03 at 298 K. Temperature dependence follows sulfuric acid aerosol.

[j] Consistent with the upper limit ≤ 0.02 from Burkholder et al. (2015)

[k] Value for α-pinene secondary organic aerosol.

[l] Eq. 12 from Bertram & Thornton (2009) with [Cl^-] = 0 because sea salt aerosol is separate. A lower limit of 0.005 is used for dry aerosol (RH < 40%). Values fall in the range 0.005-0.03.

[m] Low RH value from Thornton & Abbatt (2005). High RH value from Ammann et al. (2013). Values are for pure salt aerosol, appropriate for clean marine conditions with low organic content (Ryder et al., 2015).